

A PERFORMANCE ANALYSIS OF TRELLIS CODED MODULATION SCHEMES IN NON-INDEPENDENT RICIAN FADING CHANNELS

Chinthananda Tellambura and Vijay K. Bhargava, Fellow, IEEE
 Department of Electrical & Computer Engineering,
 University of Victoria, P.O. Box 3055,
 Victoria, B.C., Canada V8W 3P6
 email: chintha@sirius.uvic.ca
 tel (604) 721-6043, fax (604) 721-6048

ABSTRACT

This paper presents a new upper bound on the pairwise error probability (PEP) of trellis-coded modulation (TCM) schemes over nonindependent Rician fading channels. The bound is quite general, e.g., applicable to ideal coherent and pilot-tone aided detection, and differential detection, etc. Being quite accurate, the bound can be used in conjunction with a truncated union bound to estimate the bit error probability when ideal interleaving is not possible.

I. INTRODUCTION

Prompted by the current boom and the anticipated growth in mobile communication services, many authors have considered various coding strategies for mobile communication channels. The use of TCM for these systems, typically modelled as Rician or Rayleigh, yields coding gain. However, a potential for correlated channel errors exists because of the channel memory, and it is well known that TCM coding gain is realizable only for random error channels (memoryless channels). Consequently, the ordering of the transmitted symbol sequences may be permuted to randomize errors at the receiver. This operation, known as interleaving, may be implemented by using two buffers of size $N_d \times N_d$ (block interleaving) at the transmitter and the receiver. The total delay introduced limits the degree of interleaving allowable. As a result of interleaving/deinterleaving, the fading process appears to vary N_d times faster than in a noninterleaved case, i.e., the effective channel memory is now reduced to $1/N_d$ -th of before. Accordingly, a channel is said to be *ideally interleaved* if $N_d \rightarrow \infty$ and *non-ideally interleaved* if N_d is finite.

In light of the foregoing, the channel memory is reduced, but not eliminated, with non-ideal interleaving. In this work, the effect of this residual memory on the error performance of TCM, measured in terms of the bit error probability P_b , is addressed. The key to P_b estimation is the pairwise error probability (PEP), which is the probability that the decoder selects the erroneous codeword out of only two choices.

An early relevant example is Pierce and Stein [1], who present analysis of multiple-diversity performance (assuming maximal-ratio combining) for nonindependent fading among the signals. The pdf of the sum of the received powers has been obtained in terms of the eigenvalues of the covariance matrix of signals from all the diversity branches. Because of the duality between diversity methods and coding, for instance, for binary convolutional codes the PEP can be obtained similarly. For this case, Gagnon and Haccoun [2] have derived several new upper bounds.

For TCM on Rayleigh fading channels, the PEP can again be expressed in terms of the poles of the characteristic function, which in turn are the reciprocals of the eigenvalues of a weighted covariance matrix. Thus, in [3, 4] the exact PEP of a TCM

0-7803-0917-0/93\$03.00 © 1993 IEEE

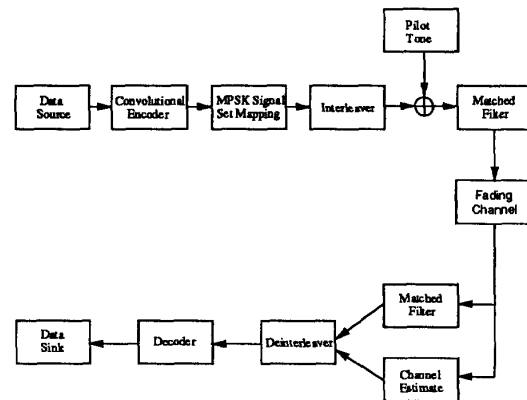


Figure 1: System Model.

scheme has been obtained by the method of residues, applicable for ideal and non-ideally interleaved Rayleigh channels. Then a truncated union bound on the bit error probability is computed using exact PEP's.

The performance analysis of coding schemes in non-ideally interleaved fading channels has been studied mostly through computer simulation rather than analysis. Some exceptions, to our knowledge, are that of [2, 4, 5]. Straightforward extension of the results in [2] to the TCM case may not be fruitful in that the Chernoff bound derived therein is known to be weak when applied to TCM schemes [3]. Likewise, the results in [4] are confined to the Rayleigh channel.

For non-ideally interleaved Rician fading channels, this paper derives a new upper bound on the PEP. Unlike in [4], the residue calculation is unnecessary, and the bound is quite general in that it can be applied to trellis-coded multilevel phase shift keying (TC-MPSK) and trellis-coded multilevel differential phase shift keying (TC-MDPSK).

The paper is organized as follows. Section II describes the system model used here and the characterisation of Rician fading channels. The bound is derived in Section III. Several examples are presented in Section IV. Conclusions are provided in Section V.

II. SYSTEM MODEL

We consider the typical system model shown in Fig. 1. Binary input data is convolutionally encoded at rate $n/(n+1)$. The encoded $n+1$ bit words are block interleaved and mapped into a sequence $\mathbf{x} = (\hat{x}_1, \hat{x}_2, \dots, \hat{x}_N)$ of M -ary PSK symbols, which constitute a normalized constellation, i.e., $x_i \in \{\exp(j2\pi k/M) : k = 0, 1, \dots, M-1\}$ for all symbols. A pilot tone is added to measure the true channel gain. The receiver deinterleaves and

©1993 IEEE. Personal use of this material is permitted. However, permission to reprint/republish this material for advertising or promotional purposes or for creating new collective works for resale or redistribution to servers or lists, or to reuse any copyrighted component of this work in other works must be obtained from the IEEE.

then applies soft-decision Viterbi decoding. Here we consider a block interleaver of N_s columns (interleaving span) and N_d (interleaving depth) rows of memory. The encoder output is written into the memory row by row and then read out column by column. The received symbols are reordered in the reverse manner.

The transmitted signal is represented in the baseband as [3]

$$e(t) = \sum_{k=-\infty}^{\infty} v_k s(t - kT_s) \quad (1)$$

where $s(t)$ is a unit-energy pulse that satisfies Nyquist's conditions for zero inter-symbol interference, T_s is the symbol duration, and

$$v_k = \begin{cases} x_k & \text{TC-MPSK,} \\ v_{k-1}x_k & \text{TC-MDPSK,} \end{cases} \quad (2)$$

where x_k denotes the k -th convolutional encoder output. Although interleaving implies that the transmitted sequence will be a scrambled version of the encoder output sequence, to simplify the notation, this effect is ignored in (1). Instead, the effect of interleaving is accounted for by modifying the channel auto-covariance function.

The signal is demodulated using a filter matched to $s(t)$. Hence, the received sample corresponding to the k -th coded symbol can be denoted by

$$y_k = \alpha_k v_k + n_k \quad (3)$$

where n_k is a complex-Gaussian random variable with zero mean and variance $\sigma^2 = (2\gamma_s)^{-1}$ where $\gamma_s = \bar{E}_s/N_0$. The channel gain α_k is modelled as a complex-Gaussian random variable having statistical parameters:

$$\langle \alpha_{k'} \rangle = A, \quad \frac{1}{2} \langle (\alpha_{k'} - A)(\alpha_{k'} - A)^* \rangle = b_0 \quad (4)$$

where the constant mean A denotes the line-of-sight (LOS) and specular components of the received signal, and b_0 is the variance of the diffuse component (Rayleigh fading) of the received signal. The normalizations $A^2 + 2b_0 = 1$ and $K = A^2/2b_0$ enable the Rician channel to be characterized by a single parameter K . Clearly, the α_k 's constitute a piece-wise constant approximation to the continuous random process $\alpha(t)$, and this approximation in effect converts the continuous random process into one with a discrete time parameter. The normalized auto-covariance function of this discrete channel is modelled as

$$\rho(\tau_1 - \tau_2) = \begin{cases} J_0(2\pi f_D N_d T_s |\tau_1 - \tau_2|) \\ \exp(-2\pi f_D N_d T_s |\tau_1 - \tau_2|) \triangleq q^{|\tau_1 - \tau_2|} \end{cases} \quad (5)$$

where f_D is the Doppler spread of the fading process and N_d is the interleaving depth. Clearly, for ideally interleaved channels, we have $N_d f_D T_s \rightarrow \infty$. Alternatively, (5) can be interpreted as indicating that the effective fade rate at the decoder is $N_d f_D$. A detailed description of this effect can be found in [4]. Other possible correlation models are given in [6].

III. PAIRWISE ERROR PROBABILITY

In the following, we derive an upper bound on the PEP when non-ideal interleaving exists. The upper bound is quite general in that it is derived for the pilot-tone concept [3, 7], which encompasses the cases such as ideal and partial coherent detection, differential detection, etc.

We assume here the availability of channel measurements: $\hat{\alpha}_k$ being an estimate of α_k . In order to evaluate the error performance, a statistical description of $\hat{\alpha}_k$ is necessary. That is, $\hat{\alpha}_k$ is Gaussian with the mean $\langle \hat{\alpha}_k \rangle$ and the variance $b_1 =$

$\frac{1}{2} \langle (\hat{\alpha}_k - \langle \hat{\alpha}_k \rangle)(\hat{\alpha}_k - \langle \hat{\alpha}_k \rangle)^* \rangle$. The normalized correlation coefficient between α_k and $\hat{\alpha}_k$ is $\mu = \frac{1}{2} \langle (\alpha_k - \langle \alpha_k \rangle)(\hat{\alpha}_k - \langle \hat{\alpha}_k \rangle)^* \rangle / \sqrt{b_0 b_1}$.

As in [3], we take the Viterbi decoder metric to be Euclidean, that is,

$$m(y_k, x_k) = -|y_k - \hat{\alpha}_k x_k|^2. \quad (6)$$

We remark that decoding with this decoding metric is not necessarily optimum for non-ideally interleaved channels. The optimum metric presumably would take into account the residual correlations. However, for ease of analysis and implementation this metric is used.

The PEP $P(\mathbf{x} \rightarrow \hat{\mathbf{x}})$ is defined to be the probability of choosing the coded sequence $\hat{\mathbf{x}} = (\hat{x}_1, \hat{x}_2, \dots, \hat{x}_N)$ when $\mathbf{x} = (x_1, x_2, \dots, x_N)$ was transmitted, given only two choices. Let $\eta \triangleq \{k_i : x_{k_i} \neq \hat{x}_{k_i}\}$ and L denote the number of elements in η , which is known as the "length" of the error event. The smallest possible L , L_{min} , is known as the code *diversity*.

The PEP, since the total metric for a codeword is the sum of component metrics, is

$$P(\mathbf{x} \rightarrow \hat{\mathbf{x}}) = \Pr\{\Xi \geq 0\} \quad (7)$$

where

$$\Xi = \sum_{i=1}^L y_{k_i} \hat{\alpha}_{k_i}^* (\hat{x}_{k_i} - x_{k_i})^* + y_{k_i}^* \hat{\alpha}_{k_i} (\hat{x}_{k_i} - x_{k_i}) \quad (8)$$

Let V_i denote the 2×1 column matrix

$$V_i = (\hat{\alpha}_{k_i} \quad y_{k_i})^T \quad (9)$$

The decision variable Ξ can then be compactly represented as

$$\Xi = \sum_{i=1}^L V_i^\dagger F_i V_i = \mathbf{V}^\dagger \mathbf{F} \mathbf{V} \quad (10)$$

where the dagger denotes conjugate transpose, and \mathbf{V} , \mathbf{F} are given by

$$\mathbf{V} = \begin{pmatrix} V_1 \\ \vdots \\ V_L \end{pmatrix}, \quad \mathbf{F} = \begin{pmatrix} F_1 & \dots & 0 \\ \vdots & \ddots & \vdots \\ 0 & \dots & F_L \end{pmatrix} \quad (11)$$

with

$$F_i = \begin{pmatrix} 0 & (\hat{x}_{k_i} - x_{k_i})^* \\ (\hat{x}_{k_i} - x_{k_i}) & 0 \end{pmatrix}. \quad (12)$$

From (3), (4) and (9), it follows that each V_i is Gaussian with mean $\langle V \rangle = (A, A x_{k_i})^T$ and the 2×2 covariance matrix

$$R_i = \begin{pmatrix} b_1 & \mu \sqrt{b_0 b_1} x_{k_i} \\ \mu^* \sqrt{b_0 b_1} x_{k_i}^* & b_0 + \sigma^2 \end{pmatrix}. \quad (13)$$

We also need the covariance matrix \mathbf{R} of the random vector \mathbf{V} . \mathbf{R} is defined as the $2L \times 2L$ matrix

$$\mathbf{R} = \frac{1}{2} \langle [\mathbf{V} - \langle \mathbf{V} \rangle][\mathbf{V} - \langle \mathbf{V} \rangle]^T \rangle. \quad (14)$$

The element of \mathbf{R} , other than those given by Eq. (13), can be obtained from Eqs. (5) and (9). For example, in the following \mathbf{R} is computed for the case of ideal channel measurements.

A. Ideal TC-MPSK

In this case it is assumed that prior measurements provide perfect channel estimation for each symbol interval. Thus, $\hat{\alpha}_k = \alpha_k$, $b_1 = b_0$, and $\mu = 1$. Assuming, without loss of generality, that the all-zero symbol sequence is transmitted, R_i can be readily obtained. To find the remaining elements of \mathbf{R} , we note that $V_i = (\alpha_i, y_i)^T$ and that the covariance between V_i and V_j ($i \neq j$, $i, j = 1, 2, \dots, L$) is

$$\frac{1}{2} \langle (V_i - \langle V_i \rangle)(V_j - \langle V_j \rangle)^T \rangle = b_0 \begin{pmatrix} \rho(|k_i - k_j|) & \rho(|k_i - k_j|) \\ \rho(|k_i - k_j|) & \rho(|k_i - k_j|) \end{pmatrix}. \quad (15)$$

A similar approach can be taken for differential detection and pilot tone aided detection [8].

B. The upper bound on PEP

To upper bound the PEP in (7), we slightly modify a lemma derived in [5].

Lemma 1 Let U be a random function, $w_U(x)$ its pdf, and $\phi_U(\omega) \triangleq \overline{\exp(j\omega U)}$ its characteristic function. Then

$$Pr[U \geq 0] < \frac{1}{2\pi} \int_{-\infty}^{\infty} \frac{|\phi_U(\alpha - j\beta)|}{\sqrt{\alpha^2 + \beta^2}} d\alpha, \quad \beta_0 > \beta > 0, \quad (16)$$

where β_0 is the boundary of the convergence region of the integral $\int_{-\infty}^{\infty} w_U(x) \exp(\beta x) dx$.

Proof: From [5]

$$Pr[U \geq 0] = \frac{1}{2\pi} \int_{-\infty}^{\infty} \frac{\phi_U(\alpha - j\beta)}{\beta - j\alpha} d\alpha, \quad \beta_0 > \beta > 0. \quad (17)$$

Since $|\int g d\alpha| \leq \int |g| d\alpha$, the lemma follows immediately. When using this lemma, one needs to know the value of β_0 , which, as will be seen next, depends on the largest positive eigenvalue of $\mathbf{R}^* \mathbf{F}$.

Now the characteristic function of Ξ (8) is given by [7, App. B]

$$G_{\Xi}(\xi) = \prod_{i=1}^{2L} \frac{1}{1 - 2j\xi\phi_i} \exp \left[\frac{j\xi\phi_i \langle \eta_i \rangle^2}{1 - 2j\xi\phi_i} \right]. \quad (18)$$

where ϕ_i , $i = 1, 2, \dots, 2L$ are the eigenvalues of $\mathbf{R}^* \mathbf{F}$. Note that \mathbf{R}^* has positive eigenvalues, but due to the structure of \mathbf{F} the matrix $\mathbf{R}^* \mathbf{F}$ has L positive eigenvalues and L negative ones. Thus, let $\phi_i < 0$ for $i = 1, 2, \dots, L$ and $\phi_i > 0$ for $i = L+1, \dots, 2L$.

To apply (16) to bound the PEP in (7), one needs the range of β , which is related to the positive poles of $G_{\Xi}(\xi)$. Since β must be less than the minimum pole on the right hand plane, the range of β is

$$0 < \beta < \left[\frac{1}{2\phi_{max}} \right] \quad (19)$$

where ϕ_{max} denotes the largest positive eigenvalue, i.e., $\max(\phi_i | i = L+1, \dots, 2L)$. Having established the range of β , we combine (7), (16), and (18) to obtain

$$P(\mathbf{x} \rightarrow \hat{\mathbf{x}}) < \frac{1}{2\pi} \int_{-\infty}^{\infty} \frac{1}{\sqrt{\alpha^2 + \beta^2}} \times \prod_{i=1}^{2L} \frac{\exp(v_i)}{\sqrt{(1 - 2\beta\phi_i)^2 + 4\phi_i^2 \alpha^2}} d\alpha \quad (20)$$

where

$$v_i = \text{Real} \left(\frac{(\beta + j\alpha)\phi_i \langle \eta_i \rangle^2}{1 - 2\beta\phi_i - 2j\alpha\phi_i} \right) \leq \frac{\beta\phi_i \langle \eta_i \rangle^2}{1 - 2\beta\phi_i}. \quad (21)$$

Thus we have

$$P(\mathbf{x} \rightarrow \hat{\mathbf{x}}) < \frac{1}{2\pi} \int_{-\infty}^{\infty} \frac{1}{\sqrt{\alpha^2 + \beta^2}} \times \prod_{i=1}^{2L} \frac{\exp \left(\frac{\beta\phi_i \langle \eta_i \rangle^2}{1 - 2\beta\phi_i} \right)}{\sqrt{(1 - 2\beta\phi_i)^2 + 4\phi_i^2 \alpha^2}} d\alpha. \quad (22)$$

In principle, we need to find the β which minimizes this upper bound, a quite difficult task. Instead, we may choose

$$\beta = \frac{1}{2} \left[\frac{1}{2\phi_{max}} \right] \quad (23)$$

and evaluate (22) numerically, again a computationally intensive task. Dividing each square root by $4\phi_i^2$, (22) can be recast as

$$P(\mathbf{x} \rightarrow \hat{\mathbf{x}}) < \Lambda(\beta) \frac{\exp[\beta \langle V \rangle^T (\mathbf{F}^{-1} - 2\beta \mathbf{R}^*)^{-1} \langle V \rangle]}{|\det(2\mathbf{R}^* \mathbf{F})|} \quad (24)$$

where

$$\Lambda(\beta) \triangleq \frac{1}{2\pi} \int_{-\infty}^{\infty} \prod_{i=0}^{2L} \frac{1}{\sqrt{(\alpha^2 + \beta_i^2)}} d\alpha \quad (25)$$

and where $\beta_0 = \beta$, $\beta_i = |(1/2\phi_i - \beta)|$ for $i = 1, 2, \dots, 2L$. Rather than integrating numerically, this integral can be bounded by applying Schwarz's inequality (for real positive functions $x(t)$ and $y(t)$, $\int x(t)y(t) dt \leq (\int x^2(t) dt \int y^2(t) dt)^{1/2}$). Splitting the integrand into two parts, squaring each part, and evaluating the two resulting integrals, we readily have

$$\Lambda(\beta) < \frac{1}{2} \left(\sum_{i=0}^L \frac{1}{\beta_i} \prod_{\substack{k=0 \\ k \neq i}}^L \frac{1}{(\beta_k^2 - \beta_i^2)} \right)^{1/2} \times \left(\sum_{i=L+1}^{2L} \frac{1}{\beta_i} \prod_{\substack{k=L+1 \\ k \neq i}}^{2L} \frac{1}{(\beta_k^2 - \beta_i^2)} \right)^{1/2}. \quad (26)$$

In deriving this, it is tacitly assumed that the β_i 's ($i = 1, 2, \dots, 2L$) are distinct. This is indeed the case for non-ideal interleaving. However, depending on the structure of an error event, with ideal interleaving, there may exist repeated eigenvalues. In this case, (26) must be modified accordingly.

Combining (24) and this, we get

$$P(\mathbf{x} \rightarrow \hat{\mathbf{x}}) < \Lambda_1 \frac{\exp[\beta \langle V \rangle^T (\mathbf{F}^{-1} - 2\beta \mathbf{R}^*)^{-1} \langle V \rangle]}{|\det(2\mathbf{R}^* \mathbf{F})|} \quad (27)$$

where Λ_1 is the upper bound on $\Lambda(\beta)$, as defined by (26). It will be shown later that this upper bound is extremely accurate, and remains so even when no interleaving is employed. Furthermore, little is to be gained by searching for the β that minimizes this bound, and, therefore, the choice (23) will be adequate.

Note that this bound can be readily used with a truncated union bound, an approach proposed by [3], to estimate the bit error probability:

$$P_b \simeq \frac{1}{n} \sum_{j=1}^N w(j) P_j(\mathbf{x} \rightarrow \hat{\mathbf{x}}) \quad (28)$$

where $w(j)$ is the number of bit errors associated with the j -th error event, and N is the maximum span of the included error events. Since the sum includes only a limited number of error events, in general, this is not an upper bound on the bit error probability.

IV. RESULTS

To see the accuracy of the bound (27), consider an error event of length two between $\mathbf{x} = (1, 1, \dots)$ and $\hat{\mathbf{x}} = (e^{j2\pi/4}, e^{j4\pi/4}, \dots)$. For Rician fading ($K = 5$ dB) with normalized Doppler 0.01, Fig. (2) depicts the exact PEP and the upper bound (27) as functions of the signal-to-noise ratio E_s/N_0 and the interleaving depth N_d . The exact PEP is computed by numerical integration of Eq. (17). It appears that the upper bound is very accurate for $P_b < 10^{-3}$. For instance, the difference between two curves can be as small as 0.2 dB asymptotically. To put this in perspective, we note that the difference between the Chernoff upper bound and the exact result for this particular error event can be 3.6 dB [3]. It is also noted that the accuracy of the bound increases as (1) K decreases, (2) $\gamma_s \rightarrow \infty$, and (3) $N_d \rightarrow \infty$. This may be explained by noting that the bound ignores the phase function of the integrand in (17).

For the same error event, the upper bound is plotted as a function of the interleaving depth N_d in Fig. 3 for auto-covariance functions: Bessel and exponential. For the exponential model, N_d is sufficient when $N_d f_D T_s \approx 0.5$, a further increase in interleaving capacity does not reduce the error probability. For the Bessel model, however, the error probability shows an oscillatory behaviour; consequently, the optimum interleaving depth for a given Doppler is now $N_d f_D T_s \approx \theta_k$ where $J_0(\theta_k) = 0$, $k = 1, 2, \dots$ and $J_0(x)$ is the zero-order Bessel function. Since these conditions hold for most error events, the overall bit error probability would behave similarly.

For Rician fading with exponential auto-covariance functions, the approximate P_b (see Eq. (28)) and simulation results are presented in Fig. (4) for the eight-state trellis code given in [9]. For simulation results, the interleaving span, N_s , is chosen to be 18 symbols. Following [4], a set of error events has been picked from the modified error state diagram, as defined by Zehavi and Wolf [10], of this trellis code. Here the set includes all error events whose span is less than or equal to 3 [4, Table I]. Simulation results and the approximate P_b agree quite well even for the no-interleaving case.

V. CONCLUSION

A tight upper bound on the PEP of a TCM scheme operating on the non-ideally interleaved Rician channel has been introduced. The bound is quite general and can be used with a truncated union bound to estimate the bit error probability. This approach may be used to obtain accurate performance estimations, thus alleviating the need for lengthy computer simulations when ideal interleaving is not possible.

REFERENCES

- [1] J. N. Pierce and S. Stein, "Multiple diversity with nonindependent fading," *Proc. IRE*, vol. 48, pp. 196-211, Oct. 1960.
- [2] F. Gagnon and D. Haccoun, "Bounds on the error performance of coding for non-independent Rician fading channels," *IEEE Trans. Commun.*, vol. 40, pp. 351-360, Feb. 1992.
- [3] J. K. Cavers and P. Ho, "Analysis of the error performance of trellis coded modulations in Rayleigh fading channels," *IEEE Trans. Commun.*, vol. 40, pp. 74-83, Jan. 1992.

- [4] P. Ho and D. Fung, "Error performance of interleaved trellis-coded PSK modulations in correlated Rayleigh fading channels," *IEEE Trans. Commun.*, vol. 40, pp. 1800-1809, Dec. 1992.
- [5] A. N. Trefimov, "Convolutional codes for channels with fading," *Prob. of Inform. Transmission*, vol. 27, pp. 155-165, Oct. 1991.
- [6] M. K. Simon, E. Biglieri, P. J. McLane and D. Divsalar, *Introduction to Trellis-Coded Modulation with Applications*. New York: McGraw-Hill, 1991.
- [7] W. R. Bennet, M. Schwartz and S. Stein, *Communication Systems and Techniques*. New York: McGraw-Hill, 1966.
- [8] C. Tellambura, Q. Wang and V. K. Bhargava, "A performance analysis of trellis-coded modulation schemes over Rician fading channels," to appear in *IEEE Trans. Veh. Technol.*, 1993.
- [9] R. G. McKay, "Error bounds for trellis-coded MPSK on a fading mobile satellite channel," *IEEE Trans. Commun.*, vol. 39, pp. 1750-1761, Dec. 1991.
- [10] E. Zehavi and J. K. Wolf, "On the performance of trellis codes," *IEEE Trans. Inform. Theory*, vol. 33, pp. 196-202, Mar. 1987.

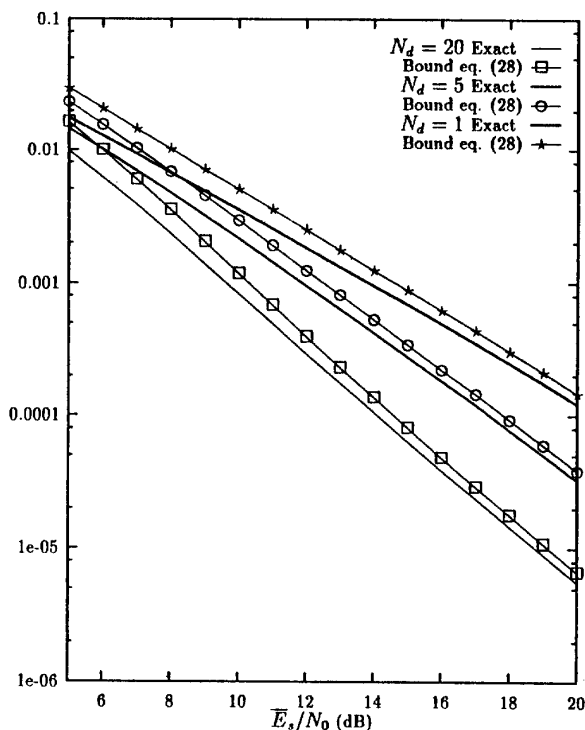


Figure 2: Exact and upper bound the PEP of an error event in a Rician fading ($K = 5$ dB) with ideal coherent detection. The normalized Doppler $f_d T_s$ is 0.01 with exponential correlation.

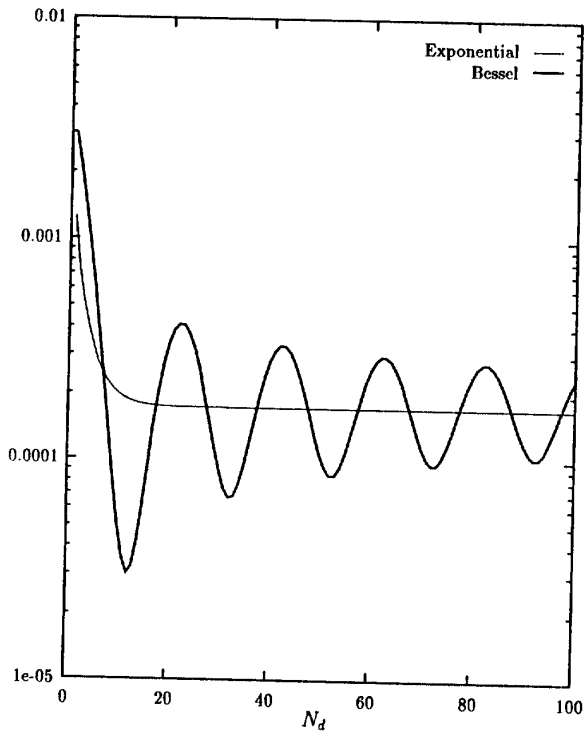


Figure 3: Upperbound on the PEP versus the interleaving depth. Rician fading ($K = 5$ dB). $\bar{E}_b/N_0 = 12.0$ dB. The normalized Doppler $f_d T_s$ is 0.05.

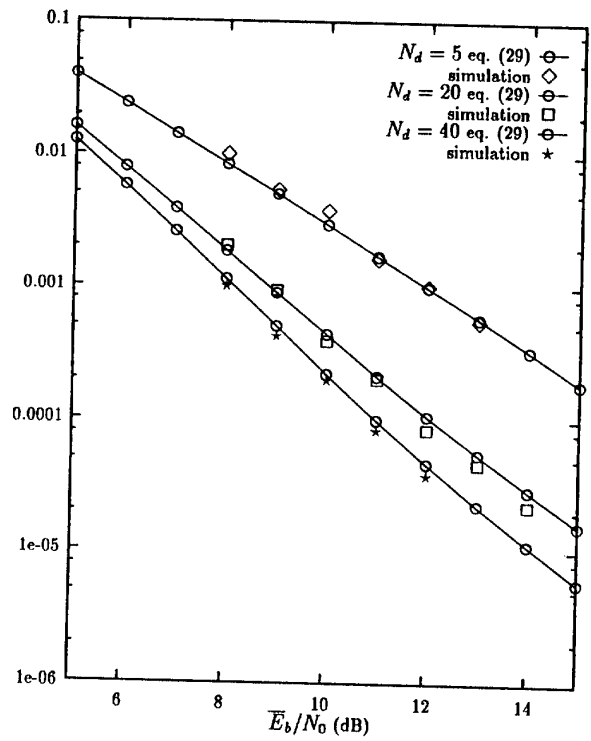


Figure 4: Simulation the approximate P_b of the 8-state trellis-code. Rician fading ($K = 5$ dB) with ideal coherent detection. The normalized Doppler $f_d T_s$ is 0.01 with exponential correlation.